Supplementary Figures

Proximal tubule–intrinsic complement shapes epithelial stress responses in rhabdomyolysis-induced acute kidney injury

Anne Grunenwald, at al

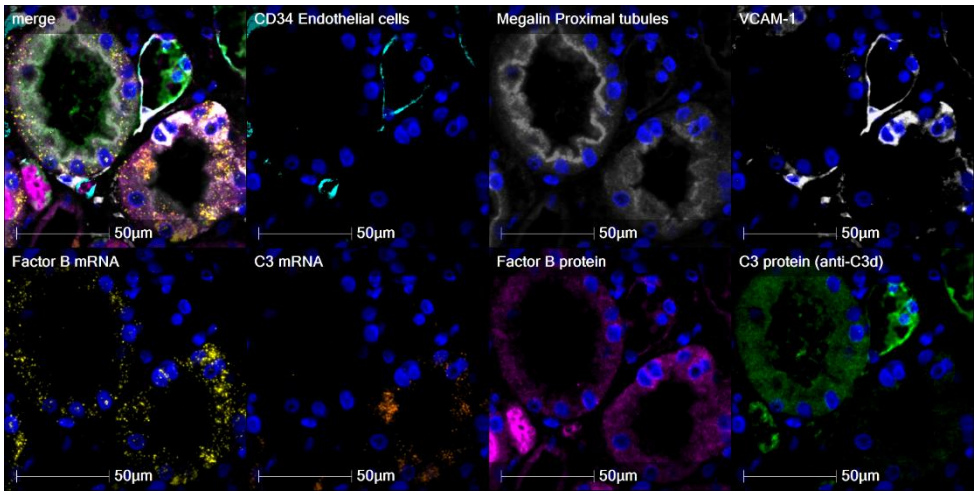

Supplementary Figure 1: C3 and FB can be both synthesized and reabsorbed by proximal tubules and their expression is associated with an inflammatory phenotype in RIAKI patients. Multiplexed sequential immunofluorescence (SeqIF) combined with RNAscope (FB and C3). Panels show merged image (top left) and individual markers (CD34: cyan, megalin : grey, VCAM-1: white, FB protein: pink, C3 protein: green, FB mRNA: yellow and C3 mRNA: orange) Examples of possible reabsorption of C3. C3 staining is not necessarily detected in proximal tubules, with detectable C3 mRNA, which could be interpreted by reabsorption of C3 from the extracellular milieu. FB and C3 staining may not be detected in the same tubules. Detection of protein and mRNA staining for C3 and FB in megalin+ proximal tubules, showing activated pattern (VCAM-1+) or not.

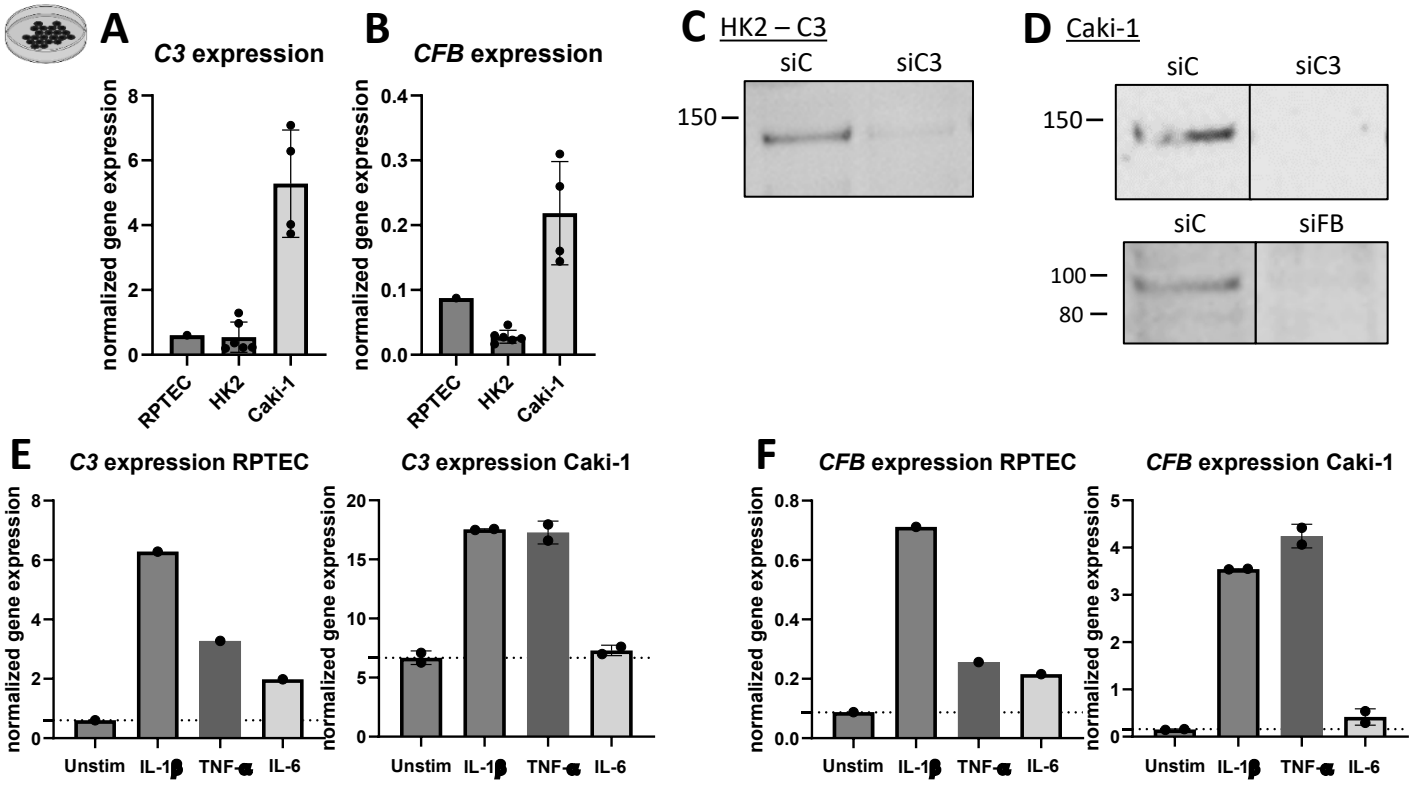

Supplementary Figure 2: C3 and FB are expressed *in vitro* by proximal tubular cells and are upregulated by inflammatory stimuli in vitro. HK2, Caki-1 and RPTEC express (A) *C3* and (B) *CFB* mRNA. (C) C3 and (D) FB were detected in the supernatants of HK2 and Caki-1 at protein level, and were efficiently knocked down by siRNA, confirming the specificity of the band. The 150 kDa band of the a-chain of C3 was detected by a polyclonal anti-C3d antibody and the 90kD band of FB was detected by an anti-FB polyclonal antibody used for the seqIF staining. (E) *C3* and (F) *CFB* gene expression is stimulated by AKI-relevant inflammatory mediators in primary proximal tubular cells from one donor (RPTEC) and in the cell line Caki-1, a model of tubular cells, derived from cancer metastasis but without VHL mutation. Gene expression detected by QuantiGene. Unstim – unstimulated cells. * $p<0.05$, Mann Whitney test for pairwise comparison.

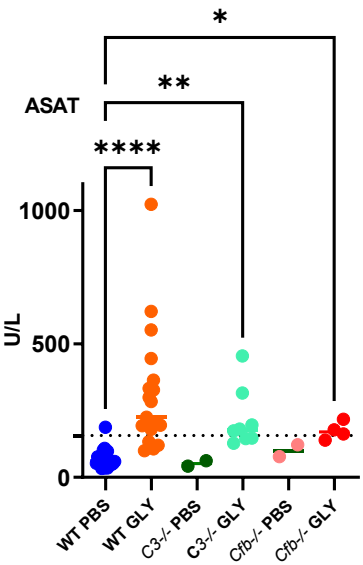

Supplementary figure 3: Evaluation of the muscle damage in the rhabdomyolysis model in WT, C3 and FB deficient mice. Muscle injury upon glycerol injection, measured by ASAT elevation occurs in (A) WT *Cfb*$^{-/-}$ and *C3*$^{-/-}$ mouse strains, exceeding the cutoff of normal level (av+2SD) of PBS injected mice, indicated as a dotted line. * p<0.05, ** p<0.01, Kruskal Wallis test with Benjamini, Krieger and Yekutieli correction for multiple comparisons.

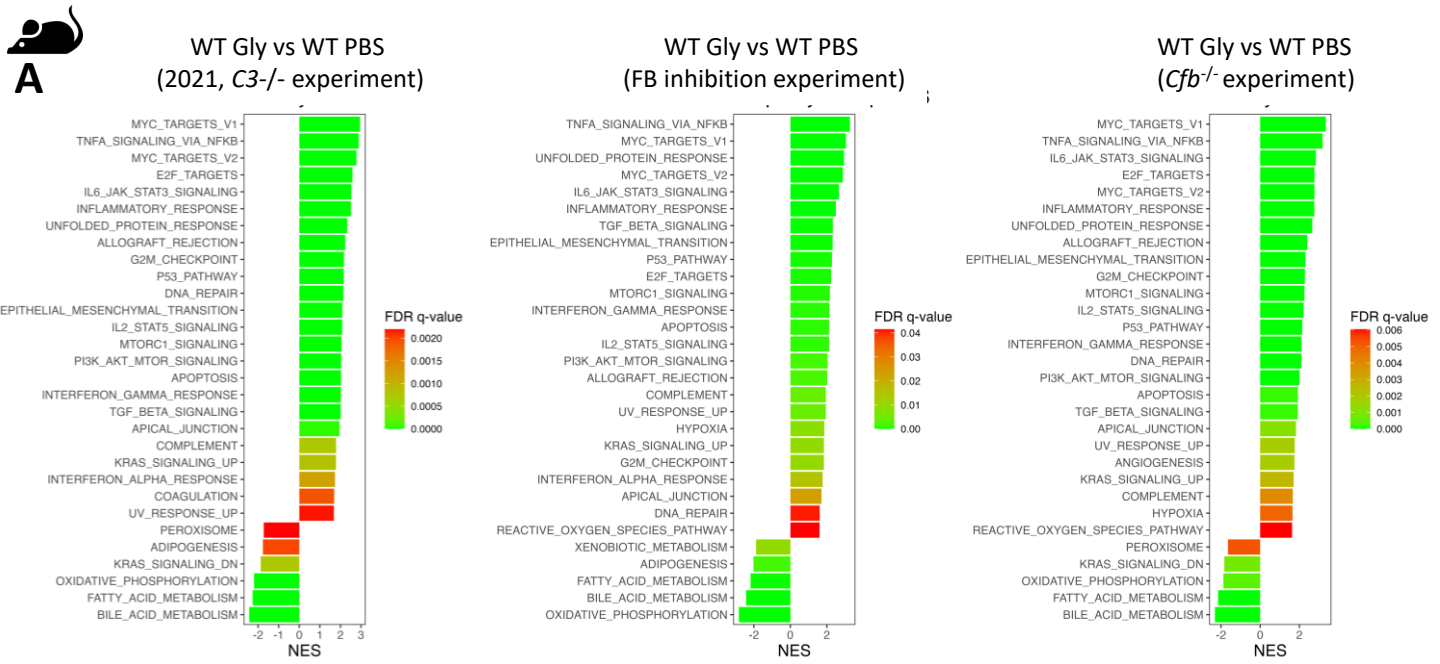

Supplementary figure 4. Gene Set Enrichment Analysis and Ligand-Receptor analysis reveal multiple maladaptive repair, fibrosis as well as complement-related pathways in mice RIAKI kidneys. A) Consistence of the RIAKI signature across different mouse experiments containing WT PBS and WT Gly (left: dataset from the *C3*$^{-/-}$ experiment from Boudhabhay et al, KI, 2021; middle: FB inhibition experiment here; right: the WT data from the *Cfb*$^{-/-}$ experiment here). Hallmarks gene sets enriched in each of the three experiments. B) Significant complement-related Ligand-Receptor interactions and C) top significant Ligand-Receptor interactions and pathways alterations in the kidney of Gly-injected mice (representative example from our dataset from 2021).

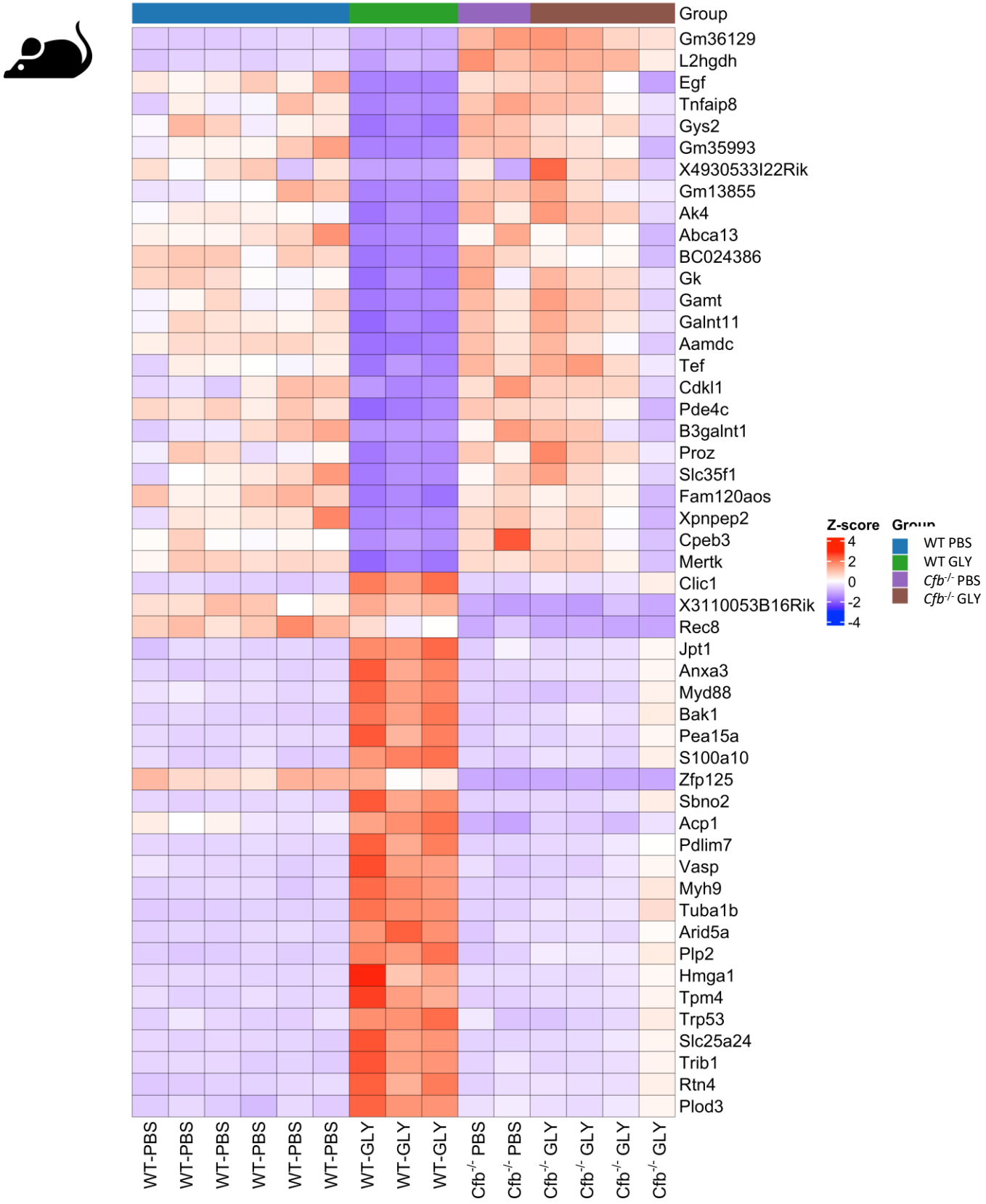

Supplementary Figure 5: Differential profiles of *Cfb*-/- mice compared to controls in presence of PBS or Gly. Heatmap of the top 50 up and down-regulated DEG in the *Cfb*-/- mice.

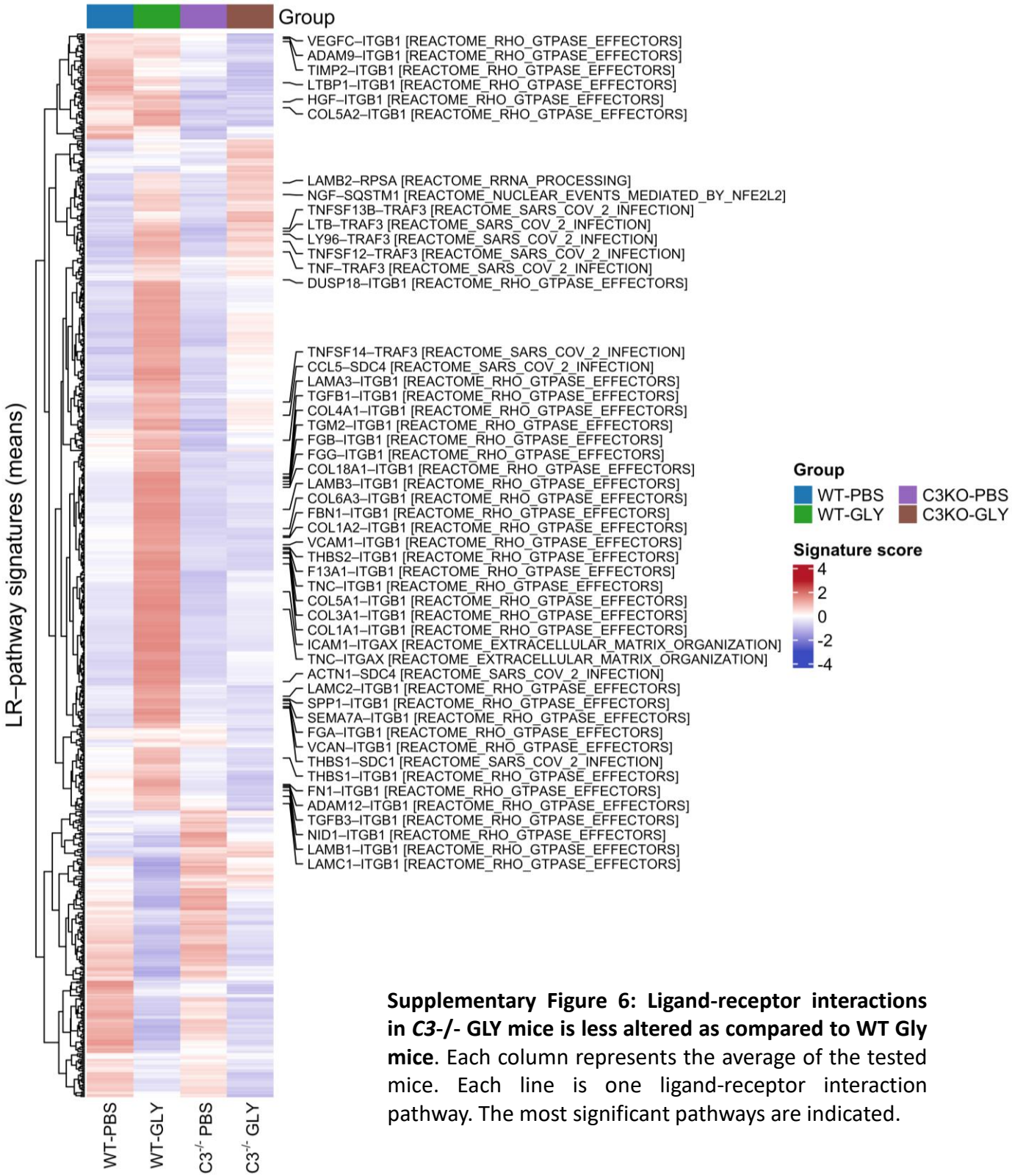

Supplementary Figure 6: Ligand-receptor interactions in *C3*-/- GLY mice is less altered as compared to WT Gly mice. Each column represents the average of the tested mice. Each line is one ligand-receptor interaction pathway. The most significant pathways are indicated.

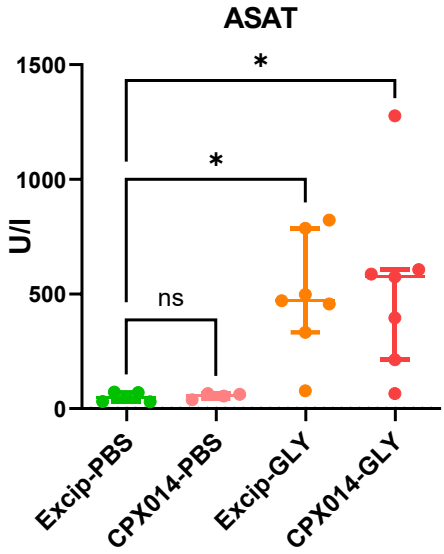

Supplementary figure 7: Evaluation of the muscle damage in the rhabdomyolysis model in WT mice, treated with CPX014. Muscle injury upon glycerol injection, measured by ASAT elevation occurs in mice treated or not with FB inhibitor CPX014 or its excipient (Excip). * $p<0.05$, ** $p<0.01$, Kruskal Wallis test with Benjamini, Krieger and Yekutieli correction for multiple comparisons.

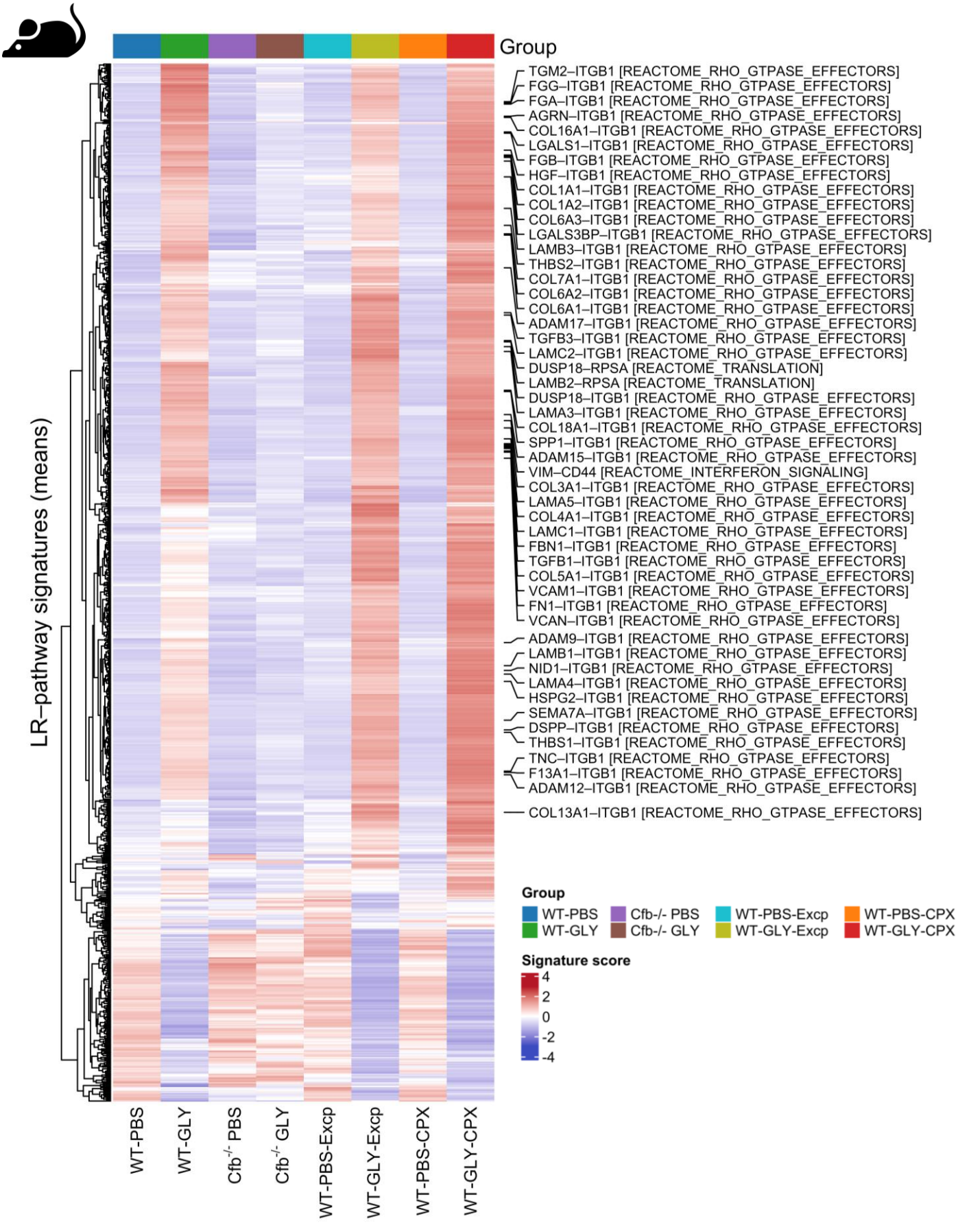

Supplementary Figure 8: Ligand-receptor interactions in *Cfb*$^{-/-}$ GLY mice are attenuated as compared to WT Gly mice but FB inhibition by CPX014 has no impact. Each column represents the average of the tested mice. Each line is one ligand-receptor interaction pathway. The most significant pathways are indicated.

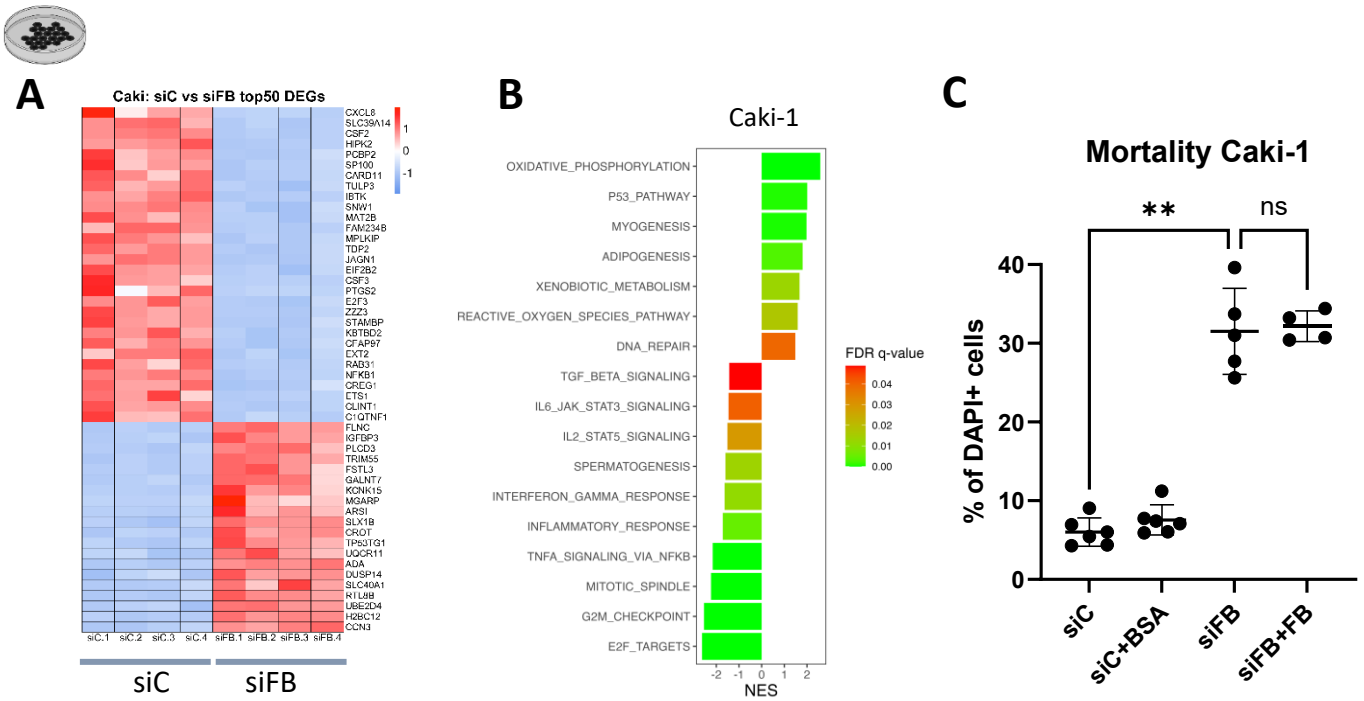

Supplementary Figure 9: Transcriptional and phenotypic changes of the FB-/- Caki-1 cells. A) Heatmap of the Top50 up and downregulated DEG in the siFB cells. B) GSEA hallmarks gene-sets impacted by FB-knockdown. Shown are the gene-sets with FDR threshold FDR<0.25 and FDR q-value p<0.05. Plotted is the Normalised Enrichment Score (NES). C) Comparison of the mortality (DAPI+ cells) for siC and siFB Caki-1 cells in presence or absence of purified FB or BSA as a control. ** p<0.01, Kruskal Wallis test with Benjamini, Krieger and Yekutieli correction for multiple pairwise comparison.

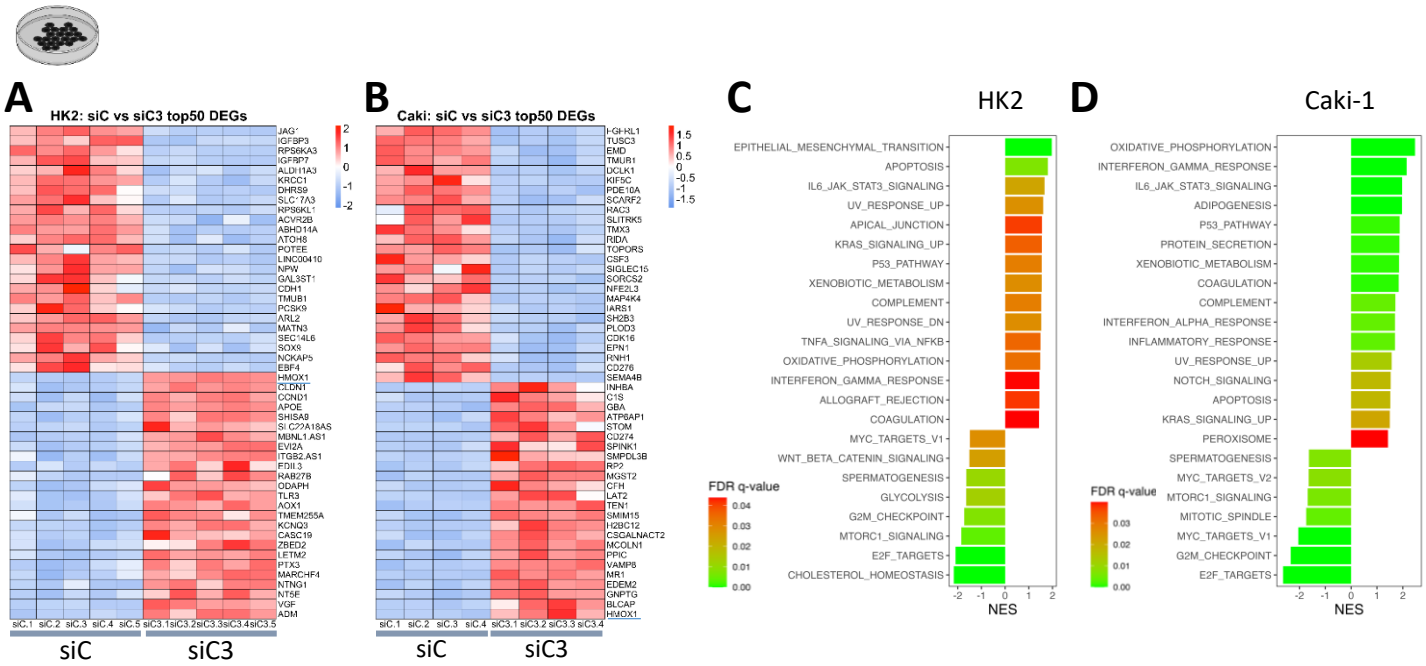

Supplementary Figure 10: Transcriptional changes of the siC3 Caki-1 and HK2 cells. (A-B) 50 top up or down DEG (absolute log fold change >1 and an adjusted p-value of less than 0,05; blue for down-regulated genes and red for up-regulating genes) in A) HK2 and B) Caki-1 cell lines. HMOX1 gene coding for the heme oxygenase 1 is underlined. (C-D) GSEA hallmarks gene-sets impacted by C3-knockdown in C) HK2 and D) Caki-1. Shown are the gene-sets with FDR threshold FDR<0.25 and FDR q-value p<0.05. Plotted is the Normalized Enrichment Score (NES).

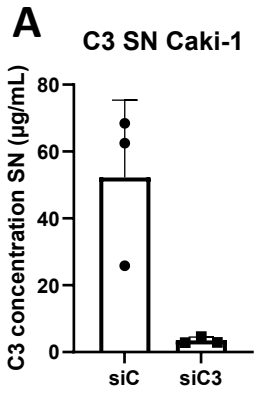
A
C3 SN Caki-1
C3 concentration SN (µg/mL)
80
60
40
20
0
siC
siC3

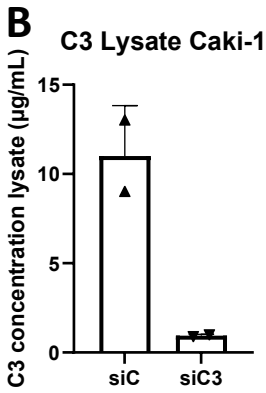
B
C3 Lysate Caki-1
C3 concentration lysate (µg/mL)
15
10
5
0
siC
siC3

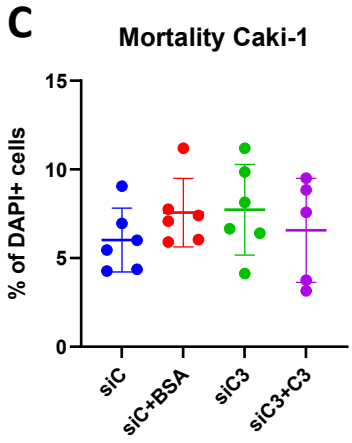
C
Mortality Caki-1
% of DAPI+ cells
15
10
5
0
siC
siC+BSA
siC3
siC3+C3

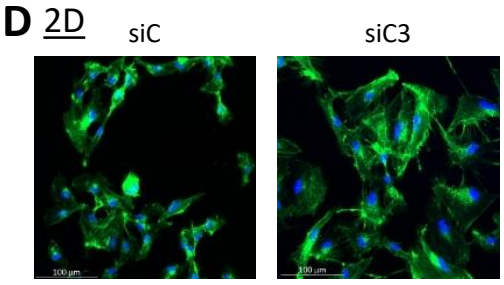
D 2D
siC
siC3

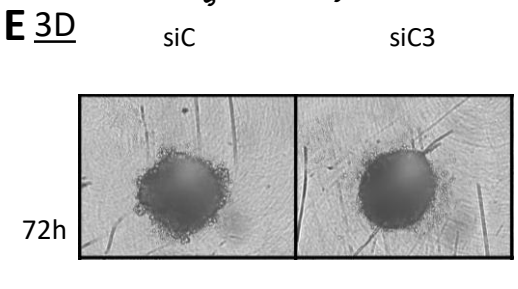
E 3D
siC
siC3
72h

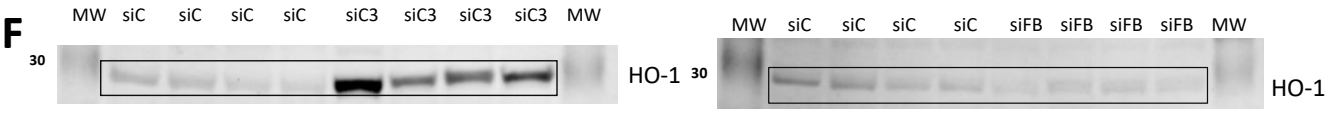
F
MW siC siC siC siC siC3 siC3 siC3 siC3 MW
30
HO-1
MW siC siC siC siC siFB siFB siFB siFB MW
30
HO-1

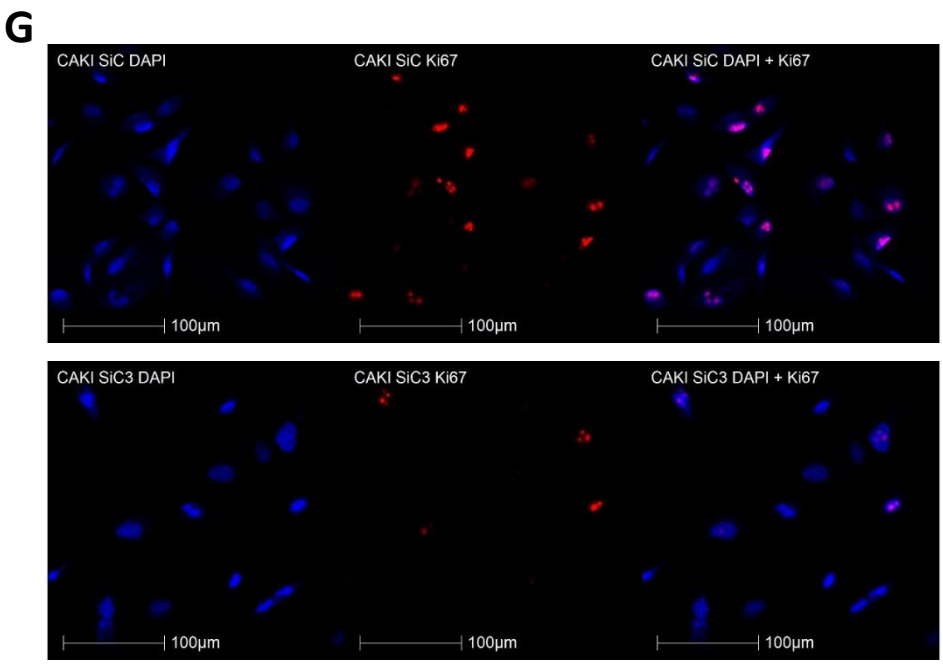
G
CAKI SiC DAPI
CAKI SiC Ki67
CAKI SiC DAPI + Ki67
100µm
CAKI SiC3 DAPI
CAKI SiC3 Ki67
CAKI SiC3 DAPI + Ki67
100µm

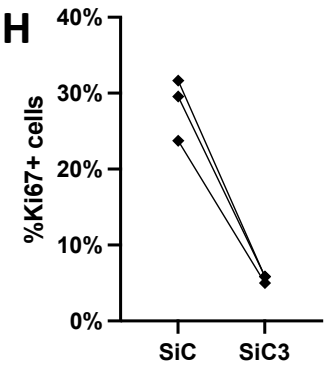
H
%Ki67+ cells
40%
30%
20%
10%
0%
SiC
SiC3

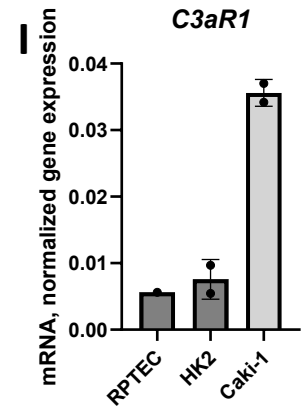
I
C3aR1
mRNA, normalized gene expression
0.04
0.03
0.02
0.01
0.00
RPTEC
HK2
Caki-1

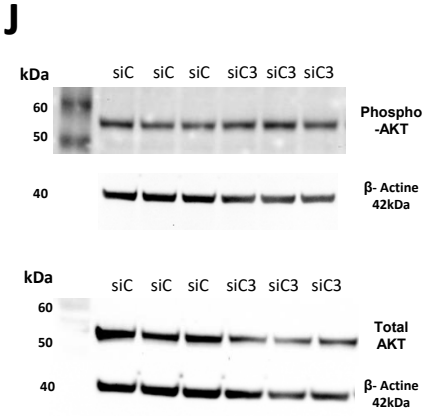
J
kDa
siC siC siC siC3 siC3 siC3
60
50
Phospho -AKT
40
β- Actine 42kDa
kDa
siC siC siC siC3 siC3 siC3
60
50
Total AKT
40
β- Actine 42kDa

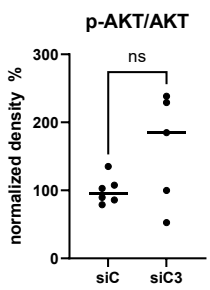
p-AKT/AKT
normalized density %
ns
300
200
100
0
siC
siC3

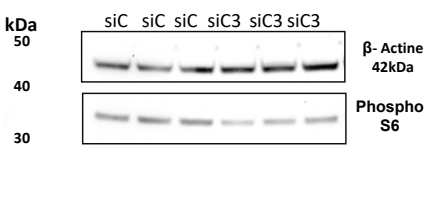
K
kDa
siC siC siC siC3 siC3 siC3
50
40
β- Actine 42kDa
30
Phospho S6

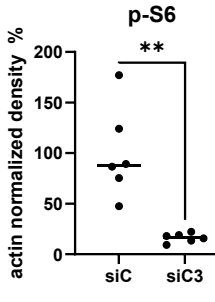
p-S6
actin normalized density %
**
200
150
100
50
0
siC
siC3

Supplementary Figure 11. C3 silencing in Caki-1 cells affects proliferation but not morphology and viability. (A-B) Detection of the presence of C3 in the A) supernatant (SN) and B) lysate, by ELISA. C) Evaluation of the cell mortality upon silencing of C3, DAPI+ cells detection by flow cytometry. (D-E) Evaluation of the overall cell capacity of form D) a monolayer in 2D cell culture and E) spheroids in 3D cell culture. F) HO-1 protein expression in siC3 or siFB Caki-1 cells compared to siC, by western blot. (G-H) Evaluation of the proliferation capacity of siC and siC3 cells by staining for Ki67, fluorescent microscopy (G) and quantification of the % of Ki67+ nuclei by Halo software (H). I) mRNA expression of *C3AR1* gene in different models of proximal tubular cells (RPTEC, primary cells, HK2 and Caki-1, cell lines). Detection by QuantiGene. J) Evaluation of AKT phosphorylation of siC and siC3 Caki-1 cells. The same cell lysate samples were deposited on two different gels, one revealed with anti-phospop-AKT and anti-actin, the second one – with anti-total AKT and anti-actin. The actin-normalized ratio of Phospho-AKT/ total AKT intensity is presented as %. K) Evaluation of S6 phosphorylation, phospho-S6 and actin were revealed on the same membrane. The actin-normalized phospho-S6 intensity is presented as %.

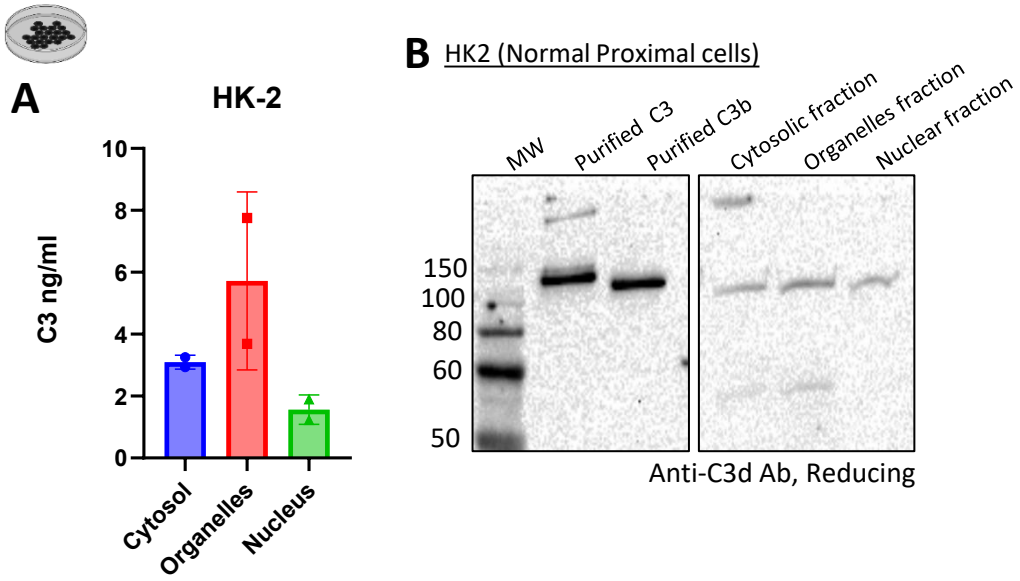

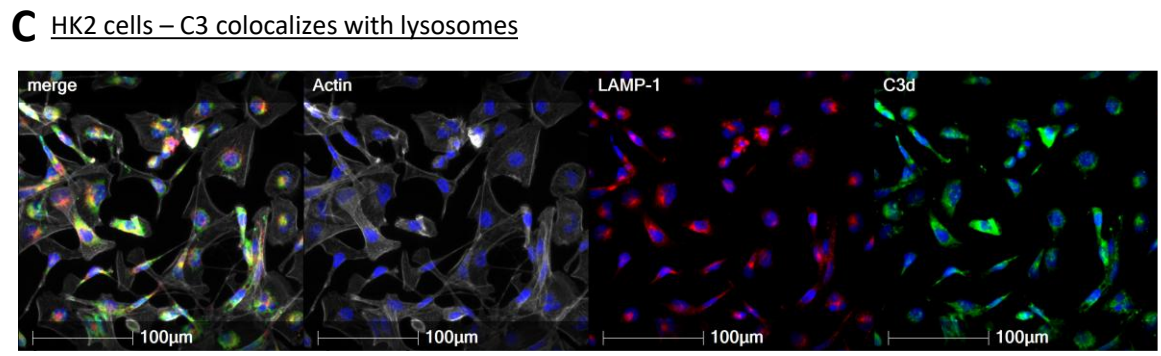

Supplementary Figure 12. Localization of intracellular C3 in HK2 cells. A-B) Detection of the presence of C3 in the sub-cellular fractions of HK2 cells A) by ELISA and B) by Western blot, using anti-C3d polyclonal antibody (does not detect the b-chain); reducing conditions. C) Colocalization of C3 staining in HK2 cells with lysosomes, revealed by fluorescent microscopy. Actin filaments were stained by phalloidin to show cell morphology (white), lysosomes are stained with LAMP1 (red), C3 staining (green).

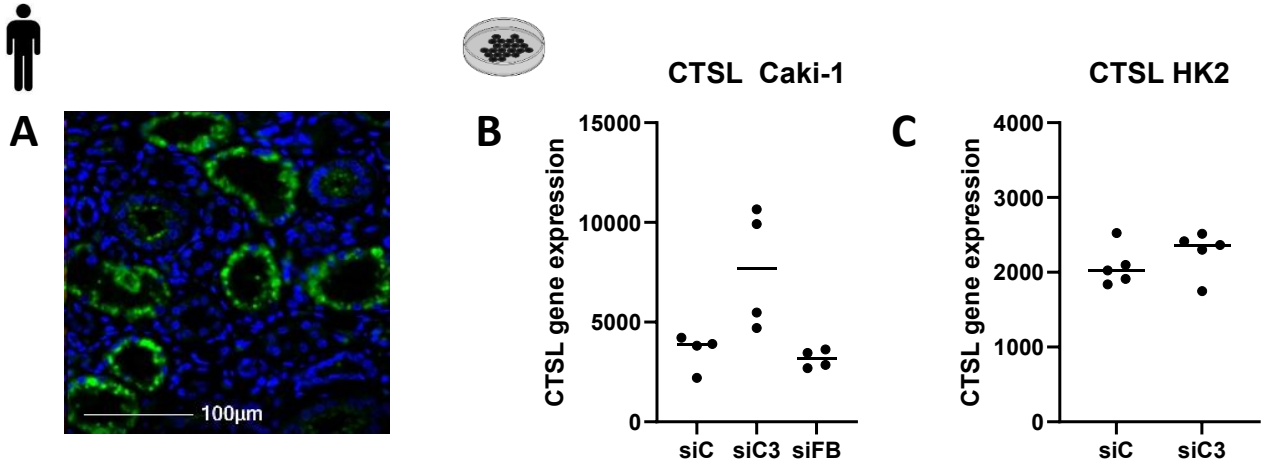

Supplementary Figure 13. Cathepsin L expression in proximal tubules. A) immunofluorescence staining of human control (peritumoral) kidney, cathepsin L is in green. B-C) *CTSL* gene expression detected by RNAseq in B) Caki-1 cells or C) HK2 cells, silenced or not for C3 or FB.